EQUIPMENT FOR THE OBSERVATION OF SOLAR NOISE AT 3,750 MC

HARUO TANAKA, TAKAKIYO KAKINUMA, HIDEHIKO JINDŌ and TOSHIO TAKAYANAGI

Abstract—A description is given of the techniques used in measuring solar noise at 3,750 MC. Problems of instrumental stability, reducing fluctuations and improving accuracy of calibration are emphasized. Some noise calculations are performed in Appendixes I and II.

I. Introduction

In the earlier part of 1950, we designed the equipment to observe 8 cm radio waves emitted from the sun. The equipment was almost completed in March 1951 and the trial observations were carried out for about 600 hours from April to July in 1951. After that, the equipment had been improved and we set about the systematic observation at the beginning of November in 1951. A considerable alteration was further carried out in August 1952. This report is the general description concerning the equipment in use at the end of 1952. Fundamental principles of this equipment are the same as those of the modulation method developed by R. H. Dicke.[1) 2) 3)]

II. Receiving Frequencies and Construction

Receiving frequency bands are as shown in Fig. 1. Two bands of microwave noise are received on both sides of the local oscillator frequency 3,750 MC (8 cm in wavelength) to improve the effective noise figure by about 3 db. Each of these bands has the bandwidth of 10 MC and is separated from the local oscillator frequency by the intermediate frequency of 60 ± 5 MC.

Block diagram of the equipment is shown in Fig. 2.

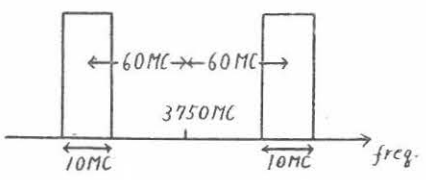

FIG. 1 (*left*). Receiving frequency bands.

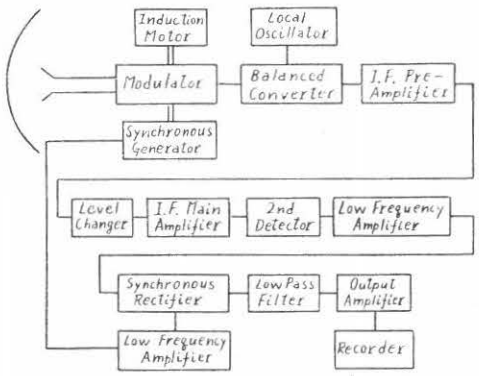

FIG. 2 (*right*). Block diagram of the equipment.

III. Microwave Equipment

1. Aerial System

Photograph of the aerial system, or radiotelescope, is shown in Photo. 1 (see 84). The antenna with a paraboloidal reflector, 2.5 m in diameter, is mounted equatorially and automatically follows the sun by means of a 8 watts synchronous motor. To reduce the influence of the radiation from the ground, the paraboloidal reflector has its focus on the aperture plane, *i.e.* its focal length is 62.5 cm. The surface of the reflector is covered with wire-nettin which has 2.8 ×2.8 mm meshes to reduce wind pressure.

The feeding horn antenna is placed at the end of the curved waveguide and its detailed structure is shown in Fig. 3. The frequency characteristic is exceedingly good, *i.e.* within 1.02 in V.S.W.R. over the entire frequency bands and, furthermore, attenuation due to raindrops is less than 1%.

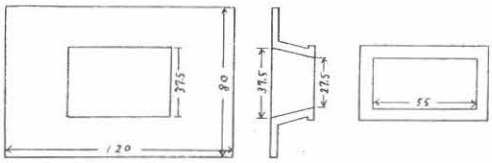

FIG. 3. Feeding horn antenna.

The receiving pattern measured with the sun as a signal source is shown in Fig. 4. The directive gain is 2,000, compared with pyramidal horn, about 2 metres in length, 379 in calculated gain.[4] But the gain is usually reduced to 1,700 by defocusing, since it is desirable that, when the sun is quiet, the effective antenna temperature comes to about 300°K in order to reduce the influence of gain variations and to facilitate calibrations.

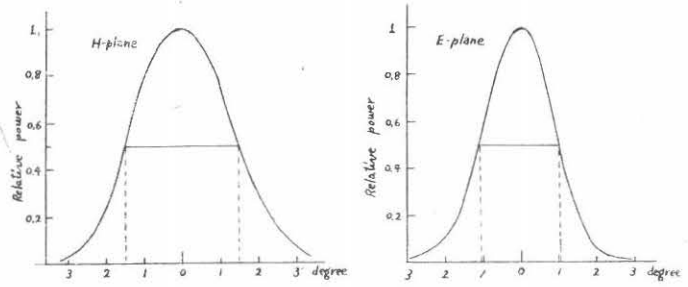

FIG. 4. Directive pattern measured with the sun as a signal.

2. Modulator

The mechanical structure of the modulator is shown in Fig. 5, which alternately connects the superheterodyne receiver to the antenna and to a resistor kept at a room temperature. The resistance of the attenuator is 150 ohm/square, maximum attenuation of which is about 35 db, and the rotating angle corresponding to the attenuation more than 10 db is 120 degrees. The V.S.W.R. for any rotating angle is below 1.1 when matched antenna is connected.

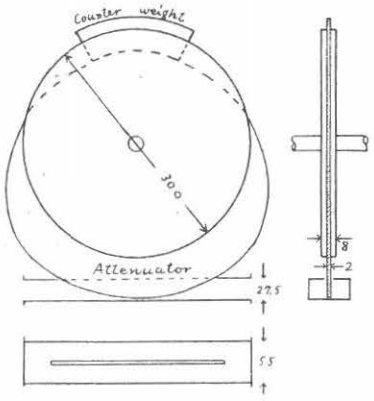

FIG. 5. Mechanical structure of the modulator.

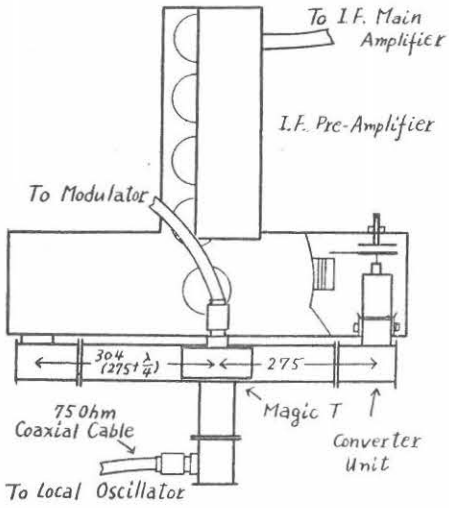

FIG. 6. Sketch of balanced converter.

3. *Balanced Frequency Converter*

A balanced frequency converter consists of a magic T, two converter units and *i-f* input circuits. Balancing should be kept over entire frequency band, otherwise appreciable error will arise in the output of a radiometer for minor change of local frequency or for the variation of the antenna impedance. A complete structure may be seen in Fig. 6, and details of the converter unit are shown in Fig. 7, the frequency response is below 1.15 in V.S.W.R. over ±60 MC. Balanced converter and *i-f* input circuits are so adjusted that no distinguishable error can be found at the recorder for the variation of antenna impedance below 1.1 in

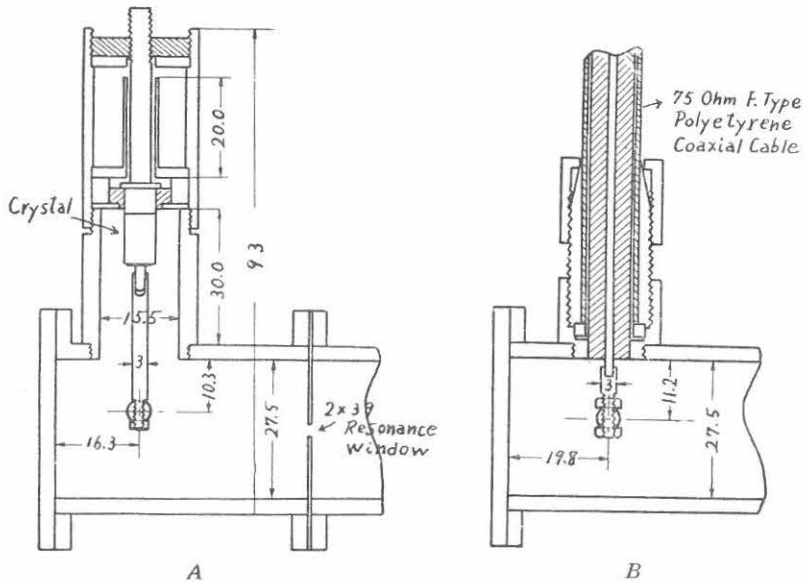

FIG. 7. Detailed structure of converter units (*A*) and coaxial cable to waveguide connection (*B*).

V.S.W.R. as well as for the variation of local frequency within 10 MC. The local oscillator is the klystron oscillator and has its regulated power supply. L.O. power is injected into E arm through a variable attenuator and a coaxial cable.

4. Protection against Mechanical Vibration

The balanced converter and *i-f* pre-amplifier in the box behind the reflector (Photo. 2, see p. 84) are supported with sponge rubbers, so that crystals, klystron and *i-f* amplifier tubes are protected from mechanical vibration due to modulator. To connect the balanced converter with the modulator, a flexible coaxial cable is used. The coaxial cable to waveguide connection is shown in Fig. 7.

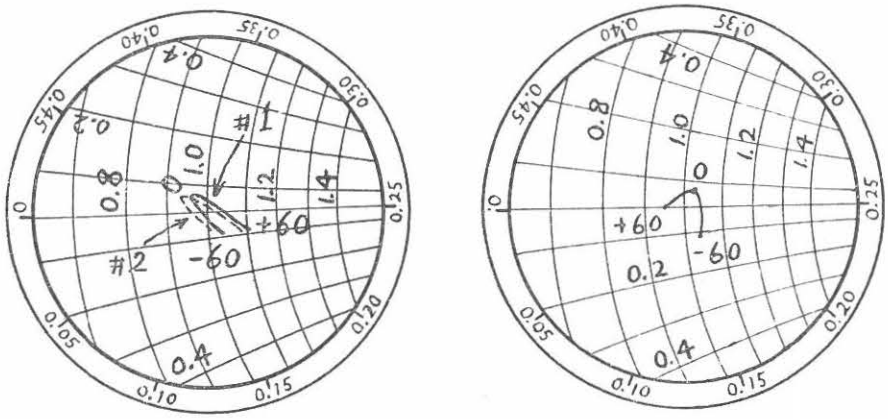

A *B*

FIG. 8. Frequency characteristics corresponding to Fig. 7.

IV. i-f Amplifier

The output fluctuation is proportional to $F/\sqrt{B_i}$ (Appendix II), where F is the

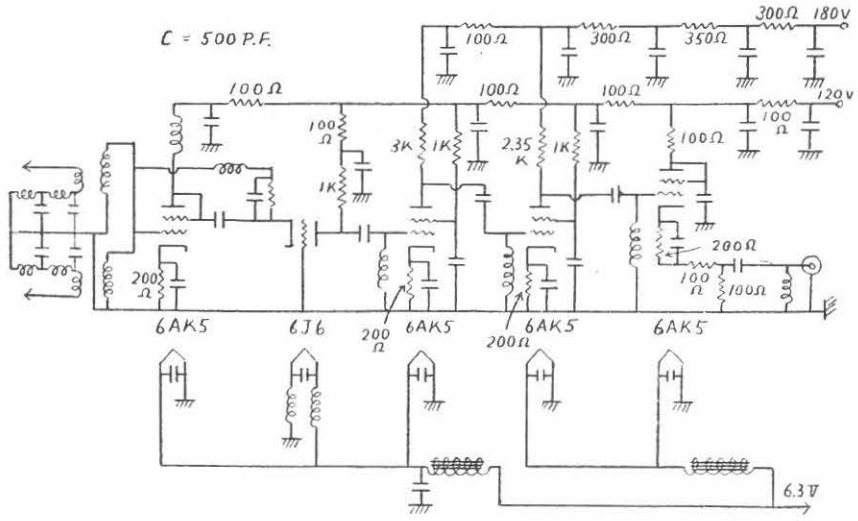

FIG. 9. *i-f* pre-amplifier.

overall noise figure and B_i is the bandwidth of the receiver. Therefore, it is desired to reduce the value $F/\sqrt{B_i}$ as much as possible.

When the crystal 1N23B and a 6AK5 cascode amplifier are used, overall noise figure may have its minimum value for the intermediate frequency around 60~100 MC. We have selected 60 MC as the centre frequency and the bandwidth of 10 MC corresponding to the minimum output capacitance of the crystal converter.

Pre-amplifier (Fig. 9) consists of a Wallmann circuit, a stagger pair and a cathode follower output. The pre-amplifier is followed by the main amplifier through a 75 ohm coaxial line and a level changer. The main amplifier (Fig. 10) consists of two stagger triple amplifiers and a diode detector. The overall gain is 105 db and is stabilized by the regulated power supply.

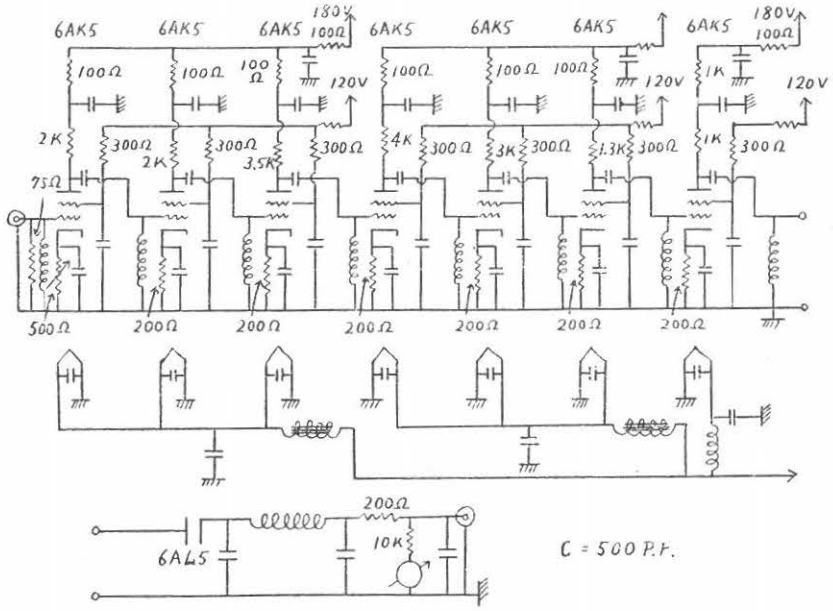

FIG. 10. *i-f* main amplifier.

V. Low Frequency Amplifier

Following the 2nd detector, a R-C selective amplifier for the modulation frequency has been used in general. But if the modulator is driven by a commercial power line, gain and phase of the amplifier will change according to the line frequency variation, as is often the case in Japan. The dependence of the amplification on the power supply frequency may be reduced by the use of a stagger amplifier, but the most radical solution is to remove selective networks. Fortunately, the results of experiences and calculations (Appendix I) show that the output fluctuations rather decrease slightly by taking these troublesome circuits away, for output signal increases more than output noise.

The schematic diagram of the low frequency amplifier is shown in Fig. 11.

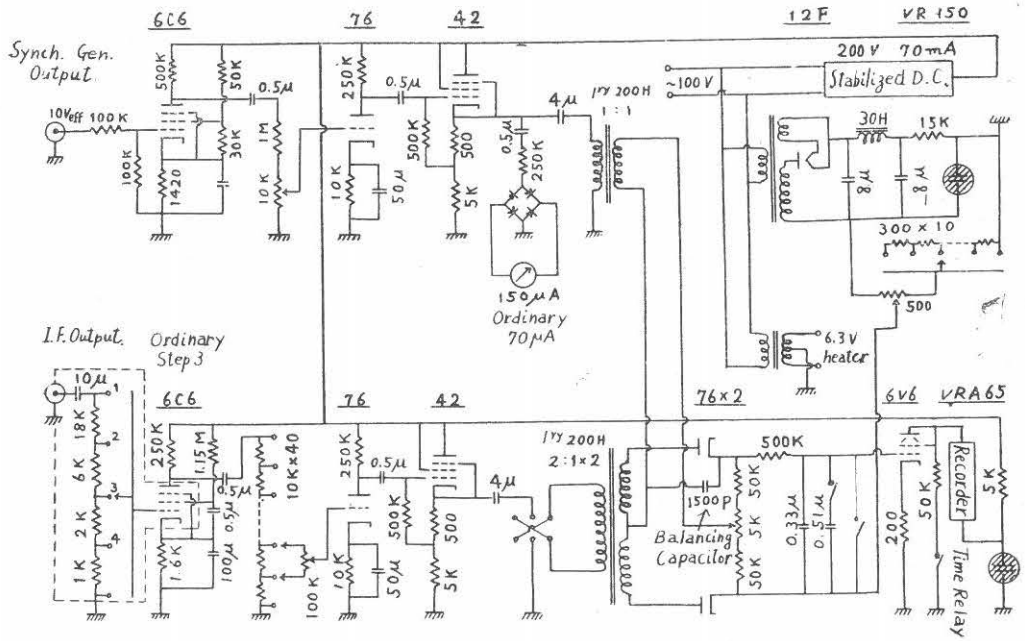

FIG. 11. Schematic diagram of low-frequency amplifier.

VI. Synchronous Rectifier

Synchronous rectifier, or the balanced mixer, as shown in Fig. 12, is simple, easy to balance and stable.

This rectifier is the gate, controlled by the square wave reference voltage, which is fed from a synchronous generator connected in series with the modulating wheel. It discriminates the phase of the signal, while it rectifies, and for adequate reference votage, linearity is kept and, in addition, minor variation of reference voltage has neglegible influence upon output voltage.

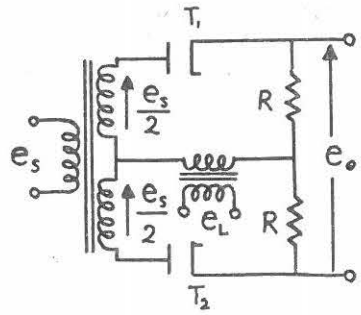

FIG. 12. Synchronous rectifier. e_0 = (either half cycle of e_s) if $|e_L| > (\text{any value of } |e_s/2|)$.

VII. Output Stage

The output stage consists of a low pass filter, output amplifier, and the recorder, as shown in Fig. 11.

The time constant of the R-C low pass filter chiefly decides the overall time constant of receiver. But the time constant of the recorder must be taken into account, in order to obtain the desired overall time constant. The overall time constant can approximately be calculated from the following equation;

$$\exp(-T/\tau) - \tau_m/\tau \exp(-T/\tau_m) = e^{-1}(1-\tau_m/\tau),$$

where τ is the time constant of the low pass filter and τ_m is that of the recorder At present, τ is 0.33 sec., τ_m is 0.15 sec. and T is 0.5 sec.

Full current of the recorder used is 10 mA. A triode connection of 6V6 tube is used as the output amplifier, which is so arranged that the current decreases as the signal at the antenna increases. Time marks are automatically inserted every one minute by shunting the tube instantaneously with a high resistance.

VIII. Power Supplies

As a matter of course, plate supply voltages as well as heating power of tubes should be stabilized as much as possible.

As the first step, the total AC power supply voltage, except that of the modulating motor, is stabilized within 100 ± 0.1 volt effective for the full load current of about 5 amperes.

Although the effective value of AC voltage is stabilized in such a way, the rectified DC voltage is not stabilized. Therefore, DC supply voltages are stabilized by conventional DC feedback stabilizers. Consequently, no appreciable change due to power line can be found in the record.

IX. 50 c/s Standard Signal Generator

In order to drive the standard clock and the driving motor of the antenna, 50 c/s standard signal generator is used. Crystal oscillator that generates 120 kc/s is followed by the frequency divider consisting of three multivibrators. The output 50 c/s controls R-C oscillator and resultant sinusoidal wave is amplified to the desired power of 32 watts.

X. Calibrations

Noise standard which may be used at microwave frequencies is confined to the thermal noise from a matched resistive termination, heated at known temperature. A radiometer can be calibrated continuously by a hot load within the range from the room temperature to about 600°K.

The sky temperature and a fluorescent lamp associated with a calibrated attenuator is useful to extrapolate the above calibration curve. In each case, errors due to substitution should carefully be avoided as discussed in the article "The Substitution Measurement of the Sky Temperature at Centimetre Waves" which may be found in this bulletin.

The effective antenna temperature when the antenna is directed towards the sky has been used as an ever ready noise substandard to correct long term or hourly alterations in sensitivity.

XI. Overall Characteristics

Equivalent antenna temperature (quiet sun)	about 280°K
Antenna gain (for ordinary solar observations)	1,700
Bandwidth	10 MC
Overall noise figure	9 db
R.M.S. fluctuation or minimum detectable equivalent antenna temperature	1°K approximately

Output variation due to the commercial power line (voltage and frequency) is negligible.

An example of the record is shown in Fig. 13.

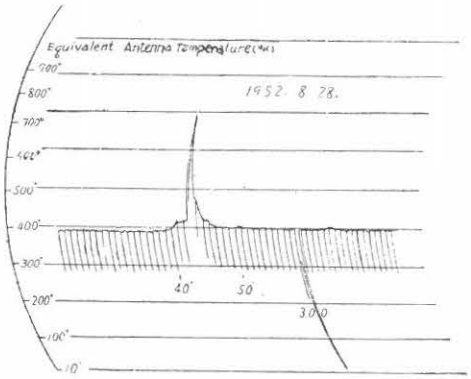

FIG. 13. An example of the record.

Appendix I

Comparison S/N Ratios Between Two Cases, When a Selective Amplifier is Used and When It is Omitted

Accurate calculation of S/N ratio will be difficult, but approximate S/N ratio can be calculated by the assumption that the noise passed through the low frequency amplifier is Gaussian. If the bandwidth of the low frequency amplifier is small compared with that of *i-f* amplifier, this assumption will hold approximately.

In order to calculate the output noise power, we must find the spectra of the noise after it has passed through a synchronous rectifier. The output noise of the low frequency amplifier may be represented as follows;

$$N(t)=\sum_{k=1}^{\infty}(a_k\cos 2\pi f_k t+b_k\sin 2\pi f_k t)\,, \tag{1}$$

where $f_k=k/\theta$ and θ is a period that is very long enough compared with any period occurring in the system. The quantities a_k and b_k are random variables and it will be assumed that,

$$\overline{a_k}=\overline{b_k}=0\,,\qquad \overline{a_k a_l}=\overline{b_k b_l}=\sigma_k^2\delta_{kl}\,,\qquad \overline{a_k b_l}=0\,.$$

As the synchronous rectifier is the gate controlled by the reference voltage, the noise amplitude after rectification can be represented as,

$$y(t)=f(t)N(t)\,, \tag{2}$$

where $f(t)$ is a function that is unity when the gate is open and zero otherwise.

To find the spectra, we calculate first the correlation function,

$$R(\tau)=\overline{y(t)y(t+\tau)}=W\cdot\rho(\tau)\frac{1}{T}\int_0^T f(t)f(t+\tau)\,dt \tag{3}$$

where $\rho(\tau)$ is the normalized correlation function of $N(t)$ and W is the total noise power, which may be represented as,

$$W=\int_0^\infty G(f)df,$$

$G(f)$ being the power spectrum of $N(t)$.

Then the spectra of $y(t)$ is represented by the equation,

$$G_0(f)=4\int_0^\infty R(\tau)\cos 2\pi f\tau\cdot d\tau. \tag{4}$$

A. When the Signal and the Reference Voltage are Symmetrical; Let $f(t)$ be a function as shown in Fig. 14,

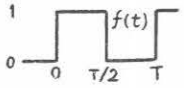

FIG. 14. Square wave function $f(t)$.

$$f(t)=\frac{1}{2}+\frac{2}{\pi}\left(\sin\omega_0 t+\frac{\sin 3\omega_0 t}{3}+\frac{\sin 5\omega_0 t}{5}+\ldots\right)$$
$$\omega_0=2\pi f_0=2\pi/T, \tag{5}$$

then

$$R(\tau)=W\cdot\rho(\tau)\left[\frac{1}{4}+\frac{2}{\pi^2}\left\{\cos\omega_0\tau+\frac{\cos 3\omega_0\tau}{3^2}+\frac{\cos 5\omega_0\tau}{5^2}+\ldots\right\}\right]. \tag{6}$$

Accordingly we have,

$$G_0(f)=\frac{W}{4}S(f)+\frac{1}{\pi^2}\cdot W\cdot S(f\sim f_0)+\frac{1}{\pi^2}W\cdot S(f+f_0)+\frac{1}{3^2}\frac{1}{\pi^2}W\cdot S(f\sim 3f_0)$$
$$+\frac{1}{3^2}\frac{1}{\pi^2}W\cdot S(f+3f_0)+\ldots, \tag{7}$$

where $S(f)=4\int_0^\infty\rho(\tau)\cos 2\pi f\tau\cdot d\tau$ is the normalized spectrum of $N(t)$.

If $S(f)$ is rectangular and has bandwidth B as shown in Fig. 15,

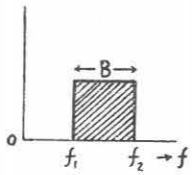

FIG. 15. Pass band of low-frequency amplifier.

$S(f)=1/B$ $\quad f_1<f<f_2$

$=0$ $\quad f_1>f,\ f>f_2.$

$S(f\sim f_0)=1/B$ $\quad f_1+f_0<f<f_2+f_0$, $f_1+f_0>f,\ f>f_2+f_0$ } when $f>f_0$.

$\quad f_0-f_1>f>f_0-f_2$, $f_0-f_1<f,\ f<f_0-f_2$ } when $f<f_0$.

$S(f+f_0)=1/B$ $\quad f_1-f_0<f<f_2-f_0$

$\quad f_1-f_0>f,\ f>f_2-f_0$

.....

a. When a selective amplifier is used; Assume that $f_0=30$, $f_2=32$, $f_1=28$, then the spectrum is represented as shown in Fig. 16.

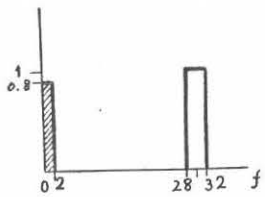

FIG. 16. Output spectrum of synchronous rectifier when a selective amplifier is used.

b. When a selective amplifier is omitted; If we assume that $f_0 = 30$, $f_1 = 1$, $f_2 = 1{,}000$ to amplify 30 c/s square wave, the spectrum is represented as the sum of those shown in Fig. 17.

From above results, the output noise power, N, can be calculated. For examp'e, the spectrum of the low pass filter, as shown in Fig. 18, will be

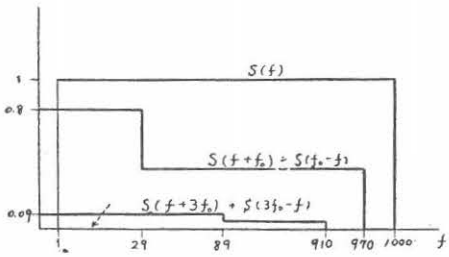

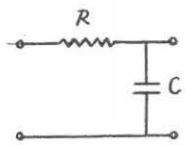

FIG. 17 (*left*). Output spectrum of synchronous rectifier when a selective amplifier is omitted.
FIG. 18 (*right*). A low pass filter, employed for example.

$$c(f) = 1/(1+f^2/b^2), \quad b = 1/2\pi RC .$$

Accordingly, the noise power will be,

$$N = \int_0^\infty G_0(f)C(f)df. \tag{8}$$

If the time constant of the low pass filter is 0.5 sec,

case a: $N \fallingdotseq 0.450\ K$,
case b: $N \fallingdotseq 0.630\ K$,

where $K = 2w/B\pi^2$.

On the other hand, as the synchronous rectifier is a halfwave rectifier for the signal, the signal power can easily be calculated. From Fig. 19,

case a: signal power $= 16A^2/\pi^4$,
case b: $= A^2/4$.

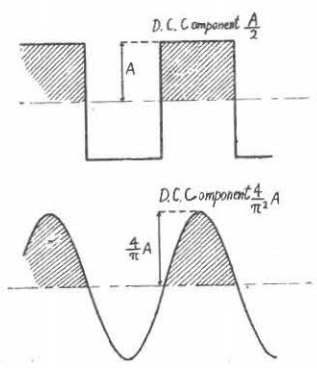

FIG. 19. Singnals of symmetrical waveform.

Accordingly, the S/N ratio is obtained as follows;

$$r_a = \text{S/N ratio in case a} = 0.365\ A^2/K,$$
$$r_b = \text{S/N ratio in case b} = 0.397\ A^2/K.$$

So $r_b/r_a = 1.09$.

S/N ratio is slightly improved when a selective amplifier is omitted.

B. When the Signal or the Reference Voltage is Asymmetrical;

c. When the signal is asymmetrical, as shown in Fig. 20, and a selective amplifier is used;

In this case, S/N ratio, $r_c = 0.274\ A^2/K$ and $r_c/r_a = 0.75$.

d. When both signal and reference voltage are asymmetrical and a selective amplifier is omitted:

When the reference voltage is asymmetrical, gate function $f(t)$ is also asymmetrical, as shown in Fig. 21.

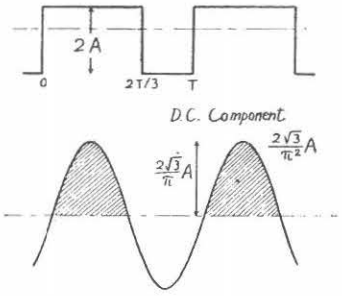

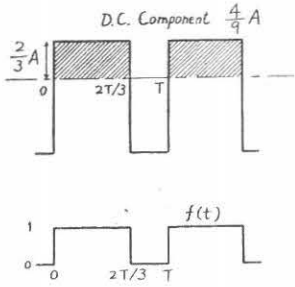

FIG. 20 (*left*). Signals of asymmetrical waveform.
FIG. 21 (*right*). Asymmetrical gate function.

In this case, the spectrum $G_0(f)$ becomes as follows;

$$G_0(f) = \frac{4}{9}W \cdot S(f) + \frac{3W}{4\pi^2}\{S(f+f_0) + S(f \sim f_0)\} + \frac{3W}{4\pi^2} \cdot \frac{1}{2^2}\{S(f+2f_0) + S(f \sim 2f_0)\} + \ldots . \qquad (9)$$

Calculating the output noise power in the same way, we have

$$N = 0.628\ K \quad \text{and} \quad r_d = 0.315\ A^2/K.$$

Comparing with case b and c, $r_d/r_b = 0.79$ and $r_d/r_c = 1.15$.

e. When the signal is asymmetrical and a selective amplifier is omitted;

In this case, the S/N ratio, $r_e = 0.176\ A^2/K$.

Comparing with case b, $r_e/r_b = 0.44$.

C. Conclusion

(1) If a selective amplifier is omitted, S/N ratio will be slightly improved.

(2) In either case, S/N ratio is largest when both signal and reference voltage are symmetrical.

(3) When the signal is asymmetrical, it is preferable to make the reference voltage the same waveform.

Appendix II

Calculations of Output Fluctuations

A. Square Law Detector

Assume that the band shape of *i-f* amplifier is square, the bandwidth is B_i and the spectral density is D. After passing through the square law detector, the noise spectrum may be expressed as shown in Fig. 22. As B_i is sufficiently large compared with the bandwidth of low frequency amplifier, the low frequency noise spectrum may be considered as uniform, *i.e.* $8B_iD^2$ in density.

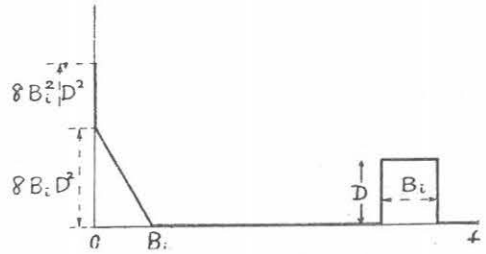

FIG. 22. Noise spectrum after passing through a square low detector.

Assume that F, θ and θ_a denote overall noise figure, room temperature and effective antenna noise temperature respectively,

$$D = a\{(F-1)\theta + \theta_a\}, \tag{1}$$

where a is a constant, proportional to the receiver gain.
Denote that $D = D_0$ at $\theta_a = \theta$, then $D_0 = aF\theta$.
Consequently, the spectral density at the output of the 2nd detector is approximately,*

$$W/B \simeq 8B_iD_0^2 = 8B_ia^2F^2\theta^2. \tag{2}$$

The signal at the output of the 2nd detector may be considered as a rectangular wave of amplitude $2A$ corresponding to the difference of D.C. component.

$$2A = \sqrt{8}B_i(D \sim D_0) = 2\sqrt{2}B_ia(\theta_a \sim \theta). \tag{3}$$

On the other hand, S/N ratio r at the output of a low pass filter has already been calculated in Appendix I and has the form,

$$r = \alpha \cdot A^2/K = \alpha\pi^2BA^2/2W. \tag{4}$$

The output noise power expressed in the equivalent antenna temperature is $\sigma_a = \theta_a \sim \theta$ when $r = 1$. So that, from the following equation derived from (4),

---

* If we take antenna side of the noise at the synchronous rectifier when selective amplifier is omitted,

$$W/B \simeq 8B_iD^2 = 8B_ia^2\{(F-1)\theta + \theta_a\}^2.$$

Accordingly, final result must be corrected as,

$$\sigma_a = 2\sqrt{2}\{(F-1)\theta + \theta_a\}/\pi\sqrt{\alpha B_i}.$$

We see that antenna side of the noise at the synchronous rectifier should be taken if $\theta_a < \theta$.

$$A^2B/W = 2/\alpha\pi^2, \tag{5}$$

we obtain,

$$\sigma_a = 2\sqrt{2}\,\theta \cdot F/\pi\sqrt{\alpha B_i}\,. \tag{6}$$

B. Linear Detector

The output spectrum of a linear 2nd detector may be expressed as shown in Fig. 23. In this case,

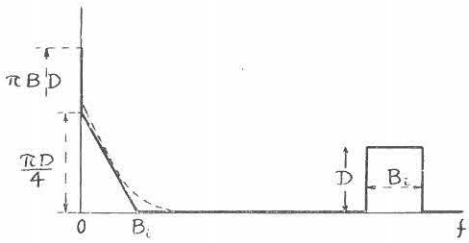

FIG. 23. Noise spectrum after passing through a linear detector.

$$2A = \sqrt{\pi B_i}\,(\sqrt{D} \sim \sqrt{D_0}) \simeq \sqrt{a\pi B_i}\,(\theta_a \sim \theta)/2\sqrt{F\theta} \quad \text{if} \quad \theta_a \sim \theta \ll F\theta. \tag{7}$$

And,

$$W/B = \pi D_0/4 = \pi a F\theta/4. \tag{8}$$

Consequently,

$$\sigma_a = 2\sqrt{2}\,\theta \cdot F/\pi\sqrt{\alpha B_i}\,, \tag{6}$$

which is the same as equation (6).

C. Comparison between these calculations and those by R. H. Dicke.

According to calculations by R. H. Dicke,

$$\sigma_a = \frac{\pi}{4}\frac{\theta}{\sqrt{T}}\frac{F}{\sqrt{B_i}}, \tag{10}$$

where T is the time constant of the low pass filter.

If $T = 0.5$ sec., $\alpha \simeq 0.37$ when a selective amplifier is employed.

R. H. Dicke or equation (10) $\quad \sigma_a \simeq 333F/\sqrt{B_i}\,.$

A, B or equation (6) $\quad \sigma_a \simeq 444F/\sqrt{B_i}\,.$

These values are not so different each other. But we can not find the relation that σ_a for the linear detector is half as much as that for the square law detector. We could not find also appreciable change in recorder fluctuation in either case, though an ordinary diode detector was not an ideal linear detector.

References

1) R. H. Dicke: The Measurement of Thermal Radiation at Microwave Frequencies. Rev. Sci. Inst. 17, No. 7 (1946).

2) Equipment Used for Recording Solar Noise at the Radiophysics Laboratory, Sydney. C.S.I.R.O., Commonwealth of Australia. Circulating Papers of Sub-Comittee Va, U.R.S.I., Jan. (1948).

3) A. E. Covington: N.R.C. 10.7 Centimeter Radiotelescope and Radiometer. N.R.C. No. 2732, Nat. Res. Cou., Ottawa, Canada, May (1952).

4) S. Silver: Microwave Antenna Theory and Design. M.I.T. Rad. Lab. Ser. 12, Chap. 15, Sec. 21.

5) J. L. Lawson and G. E. Uhlenbeck: Threshold Signals. M.I.T. Rad. Lab. Ser. 24, Chap. 3 and 9.

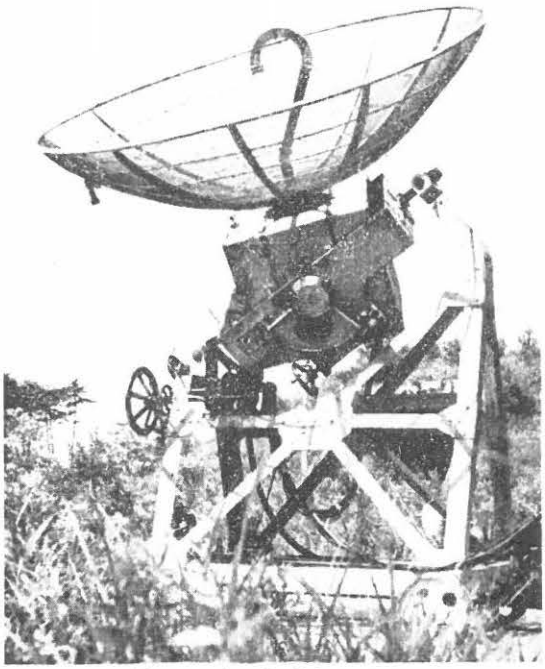

PHOTO. 1. Aerial system.

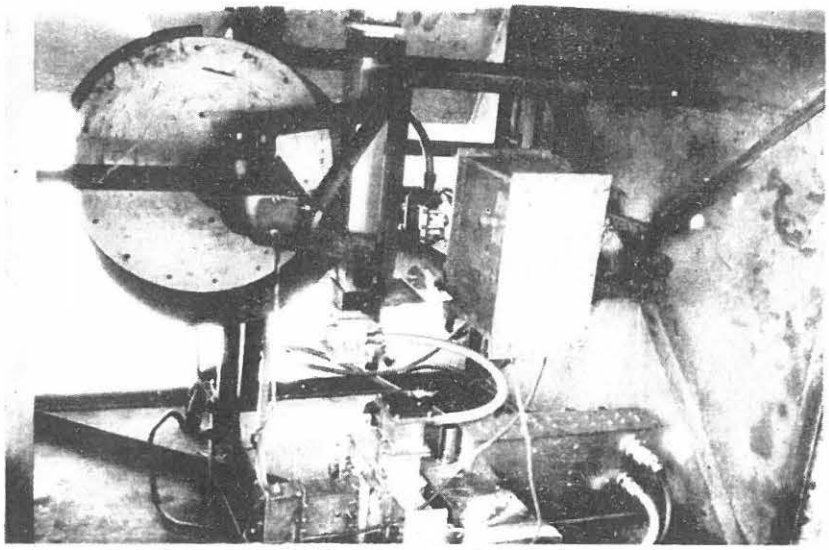

PHOTO. 2. Inside of the box behind the reflector.